International Journal of Innovative
Computing, Information and Control
Volume **7**, Number **5(B)**, May **2011**

ICIC International ©2011 ISSN 1349-4198
pp. **2739–2753**

CAPACITY OPTIMIZATION OF THE SUPERCAPACITOR ENERGY STORAGES ON DC RAILWAY SYSTEM USING A RAILWAY POWERFLOW ALGORITHM

Hansang Lee[1], Jiyoung Song[1], Hanmin Lee[2], Changmu Lee[2]
Gilsoo Jang[1] and Gildong Kim[2]

[1]School of Electrical Engineering
Korea University
Anam-Dong 5-Ga, Seongbuk-Gu, Seoul 136-701, Republic of Korea
{ hansang80; riddle23; gjang }@korea.ac.kr

[2]Advanced EMU Research Team
Korea Railroad Research Institute
360-1, Woulam-Dong, Uiwang-City, Gyeonggi-Do 437-757, Republic of Korea
{ hanmin; cmlee; gdkim }@krri.re.kr

Received February 2010; revised June 2010

Abstract. *The electric railway system is one of the most peculiar power systems of which the location and power of electrical load are continuously variable. The variance of the location and power of the vehicle changes the participation factor of each substation for the vehicle and the sign and magnitude of the load current, respectively. Especially, on the substation feeder, there is huge voltage fluctuation generated by the regenerative energy due to the braking vehicles. This regenerative energy is closely related with the energy efficiency since the surplus energy cannot be utilized and dissipated in the resistor. To improve energy efficiency of the railway system and utilize the surplus regenerative energy, the application of energy storage has been studied. In this paper, a DC railway powerflow algorithm considering storages is developed to analyze the railway system with storages and to calculate the optimal power and storage capacity of them. The Seoul Metro Line 7 is selected for the test system and simulated to verify the effect of storages. Also, the optimal power and storage capacity of each SCES is calculated.*

Keywords: DC electric railway system, Railway powerflow algorithm, Regenerative energy, Energy storage system (ESS), Supercapacitor energy storage (SCES), Energy efficiency improvement

1. **Introduction.** A number of researches to overcome energy crisis against the exhaustion of fossil fuel, environmental pollution and global warming have been performed. Typically, a number of studies on renewable energy, such as wind, photovoltaic generation, etc., are actively in progress. These types of generation have advantages that they do not use fossil fuel as an energy source and emit greenhouse gas [1-4]. The other types of these researches against energy crisis are to reduce energy consumption or loss which deals mainly with how to improve energy efficiency. As a means of efficiency improvement, various types of energy storage devices are being spotlighted and their application studies are making progress over the wide range of power systems [5,6].

Over the whole power system, researches about energy storage and its application scheme to retrench energy consumption and to enhance system efficiency are under progress. For example, on high-speed driving, hybrid car drives motors as generators to store electrical energy on energy storage device, such as batteries or super capacitors. On low-speed driving, it obtains energy not from the gasoline engines but from storage.

Similarly with the hybrid car, energy storage application researches on the electric railway systems have been progressed accordingly. The electric railway system has a peculiar characteristic that the railway vehicles need huge electric power on acceleration and supply regenerative power on braking. Although the regenerative power can be utilized in the adjacent accelerating vehicles, most of the energy, which is being unutilized, is dissipated on the feeder and vehicles in the form of thermal loss. Especially, since each electric railway vehicle repeats the operation of the accelerating and braking between every two stations, it is expected that the amount of the dissipated energy by heating is a considerable amount on a daily basis [7].

As mentioned before, since the energy storage systems are good for improving energy efficiency in the electric railway systems due to frequent repetition of acceleration and braking of vehicles, there are a number of researches about ESSs' application [8]. Especially, most of research suggests the on-board type storage which installs ESSs in each railway vehicle [9]. In the aspect of loss, it can be expected that the on-board type storage has best performance since this type can eliminates the thermal loss generated when the regenerative current flows between vehicle and substation [10,11]. However, when considering the cost of storage and energy conversion system and the maintenance cost of a number of ESSs, substation-installed ESSs are more economic. Therefore, this paper suggests the substation-installed ESSs and the algorithm to determine the capacity of that type of storage.

Section 2 addresses the base equations for railway powerflow and introduces how the energy storage in railway system can be considered. Also, the optimization method to determine the power and energy capacity of storages is addressed. Section 3 describes the configurations of the Seoul Metro line 7 which is selected as the test system. The case studies and analysis are described in Section 4. The final analysis and conclusions are presented in Section 5.

2. DC Railway Power Algorithm with Considering SCES.

To analyze the effects of SCES, it is essential to develop the powerflow algorithm which can consider the movement and the power variation of the vehicles. This section introduces the time-interval powerflow algorithm for the electric railway system and suggests the electric and mechanical analysis to get powerflow solutions. Also, this section suggests the methodology to consider SCESs with the algorithm.

The general circuit analysis method obtains solutions from the loop equations or nodal equations. Since the method based on the nodal equations is systematic and easy to build, it is mainly used for computer analysis. For the pre-existing powerflow analysis on the electric railway systems, there have been two types of methodology. In the case of non-grounded railway systems, the analysis has been performed by building a ladder circuit Jacobian matrix, applying the chain-rule reduction, and then performing iterative calculations [12]. In the case of grounded systems, solutions can be obtained by solving the Norton equivalent parameters for railway substations, building nodal equations and making iterative calculations. For the DC railway powerflow algorithm in this paper, since the Korean railway system is a grounded type, the latter type of calculation was applied. Additionally, in order to acquire more accurate simulation results, this algorithm considers not only the feeder impedance but also the rail impedance between the substation and railway vehicle [13,14].

2.1. Nodal equations.

Figure 1 illustrates the equivalent circuit of the simple railway system which is composed of 1 railway vehicle and 2 substations with supercapacitor. SCESs are modeled by current injection models and so the nodal equation can be written

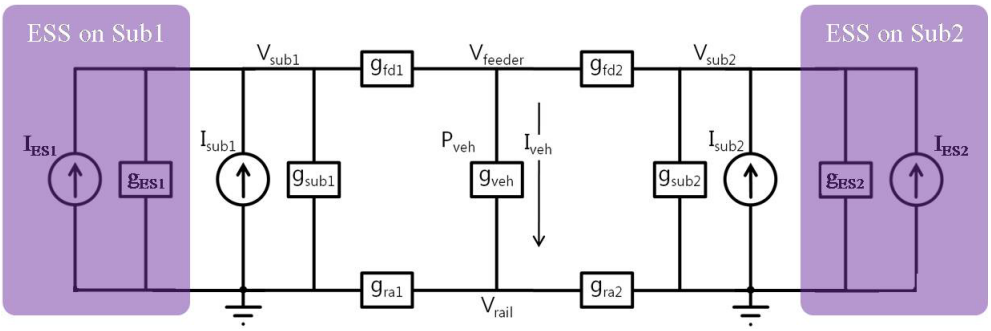

FIGURE 1. Norton equivalent circuit for the simple railway system

as Equation (1). Equation (1) appears to be a set of 1st order simultaneous equations. However, since the vehicle loads are not constant impedance loads but constant power loads, the equivalent vehicle conductance, g_{veh}, cannot be regarded as a fixed value. Since the relation between P_{veh}, g_{veh}, and the vehicle voltage can be defined as shown in Equation (2), the solution of Equation (1) should be obtained by using iterative calculations. Also, in each iteration step to solve Equation (1), the conductance matrix should be updated with the updated equivalent vehicle conductance. This has the drawback of a slow convergence speed.

$$\begin{bmatrix} g_{sub1}+g_{fd1}+g_{ES1} & 0 & -g_{fd2} & 0 \\ 0 & g_{sub2}+g_{fd2}+g_{ES2} & -g_{fd2} & 0 \\ -g_{fd1} & -g_{fd2} & g_{fd1}+g_{fd2}+g_{veh} & -g_{veh} \\ 0 & 0 & -g_{veh} & g_{ra1}+g_{ra2}+g_{veh} \end{bmatrix} \begin{bmatrix} V_{sub1} \\ V_{sub2} \\ V_{feeder} \\ V_{rail} \end{bmatrix} = \begin{bmatrix} I_{sub1}+I_{ES1} \\ I_{sub2}+I_{ES2} \\ 0 \\ 0 \end{bmatrix} \tag{1}$$

$$g_{veh} = \frac{P_{veh}}{(V_{feeder}-V_{rail})^2} \tag{2}$$

In order to overcome the calculation complexity and to improve the slow convergence speed, it is suggested that the electric railway vehicle be substituted by an equivalent vehicle current value, I_{veh}, which can be called as the current-equivalent iterative method. Since Equation (3) presents the relation between the vehicle voltage, equivalent vehicle current and equivalent vehicle conductance, Equation (1) can be substituted by Equation (4). Equation (5) presents the relation between voltage, current and power. Since this method updates only the current vector, the calculation time can be reduced significantly comparing with the conductance-equivalent iterative method.

$$I_{veh} = g_{veh} \cdot (V_{feeder} - V_{rail}) \tag{3}$$

$$\begin{bmatrix} g_{sub1}+g_{fd1}+g_{ES1} & 0 & -g_{fd2} & 0 \\ 0 & g_{sub2}+g_{fd2}+g_{ES2} & -g_{fd2} & 0 \\ -g_{fd1} & -g_{fd2} & g_{fd1}+g_{fd2} & \\ 0 & 0 & & g_{ra1}+g_{ra2} \end{bmatrix} \begin{bmatrix} V_{sub1} \\ V_{sub2} \\ V_{feeder} \\ V_{rail} \end{bmatrix} = \begin{bmatrix} I_{sub1}+I_{ES1} \\ I_{sub2}+I_{ES1} \\ -I_{veh} \\ I_{veh} \end{bmatrix} \tag{4}$$

$$I_{veh} = \frac{P_{veh}}{(V_{feeder} - V_{rail})} \tag{5}$$

In Equation (4), the equivalent source conductance, g_{sub}, can be found by on-site measurement. However, the equivalent storage conductance, g_{ES}, is hard to determine since it is dependent on the power capacity of its power conversion system. Therefore, based on that the conductance participates in the storage loss, it is assumed that the SCESs have 95% energy efficiency in this algorithm. This 95% efficiency is converted to the coefficient which is 1.0 for charging current or 0.95 for discharging current.

If the railway system without any SCES is considered, since the each storage current, I_{ES}, is zero, Equation (4) can be solved easily. However, in the case with SCESs, the Equation (4) should be modified since the substation voltages are fixed on upper or lower limit voltage. Therefore, to solve the required additional current from the storage devices, any specific substation voltage term should be moved to the right side. Instead, the substation current, which was a constant value, now becomes a variable term and should be moved to the left side. In order to exchange their position, the algorithm uses a 'variable swapping' function.

Assuming that the ith substation voltage surpasses the limits, the ith components, V_{sub_i} and $I_{sub\_i} + I_{ES\_i}$, should be swapped in order to find the additional current, I_{ES_i}, which is from/to the SCES. For that specific substation, the conductance matrix should be reconstructed using Equation (6). It is time-consuming to swap the variables for several substations simultaneously, since a row and column vector substitution and an inverse matrix construction are required for this process. The algorithm in this paper swaps the variables one at a time in order of precedence to avoid any redundant processes. Based on the reconstructed conductance matrix obtained by the variable swapping processes, the algorithm finds the storage-considered solution through the iteration.

$$\begin{bmatrix} \mathbf{G}_{11} & \mathbf{G}_{1i} & \mathbf{G}_{12} \\ \mathbf{G}_{i1} & g_{ii} & \mathbf{G}_{i2} \\ \mathbf{G}_{21} & \mathbf{G}_{2i} & \mathbf{G}_{22} \end{bmatrix} \begin{bmatrix} \mathbf{X}_1 \\ x_i \\ \mathbf{X}_2 \end{bmatrix} = \begin{bmatrix} \mathbf{Y}_1 \\ y_i \\ \mathbf{Y}_2 \end{bmatrix} \Rightarrow$$

$$\begin{bmatrix} \mathbf{G}_{11} - \frac{\mathbf{G}_{1i} \cdot \mathbf{G}_{i1}}{g_{ii}} & \frac{\mathbf{G}_{1i}}{g_{ii}} & \mathbf{G}_{12} - \frac{\mathbf{G}_{1i} \cdot \mathbf{G}_{i2}}{g_{ii}} \\ -\frac{\mathbf{G}_{i1}}{g_{ii}} & \frac{1}{g_{ii}} & -\frac{\mathbf{G}_{i2}}{g_{ii}} \\ \mathbf{G}_{21} - \frac{\mathbf{G}_{2i} \cdot \mathbf{G}_{i1}}{g_{ii}} & \frac{\mathbf{G}_{2i}}{g_{ii}} & \mathbf{G}_{22} - \frac{\mathbf{G}_{2i} \cdot \mathbf{G}_{i2}}{g_{ii}} \end{bmatrix} \begin{bmatrix} \mathbf{X}_1 \\ y_i \\ \mathbf{X}_2 \end{bmatrix} = \begin{bmatrix} \mathbf{Y}_1 \\ x_i \\ \mathbf{Y}_2 \end{bmatrix} \tag{6}$$

2.2. **SCES operating voltage optimization.** In order to utilize the regenerative energy efficiently, this section presents an algorithm that determines the optimized feeder voltage control range for the charging-discharging of the SCES in order to maximize the improvement of energy efficiency and minimize the total storage capacity. As shown in Figure 2, SCESs are designed to operate in the charging, storing, or discharging mode by sensing the substation feeder voltage, V_{sub} [15]. Since the Korean suburban railway system is a DC system, the V_{sub} is largely influenced by the supplying and regenerative power [13]. In this section, the optimization algorithm which determines the charging and discharging voltage of SCESs is being proposed.

2.2.1. *Charging voltage determination.* Figure 3 illustrates the DC voltage of the railway substation of which the no-load voltage ($V_{no-load}$) is 1,650V. Since the regenerative energy entirely causes that V_{sub} becomes higher than $V_{no-load}$, the charging voltage ($V_{charging}$) should not be set higher than $V_{no-load}$. Unless, the regenerative power corresponding to 'Area A' in Figure 3 cannot be utilized.

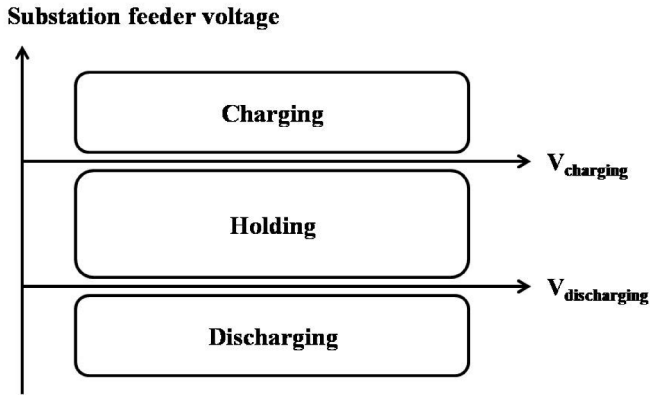

FIGURE 2. SCES operation by the feeder voltage

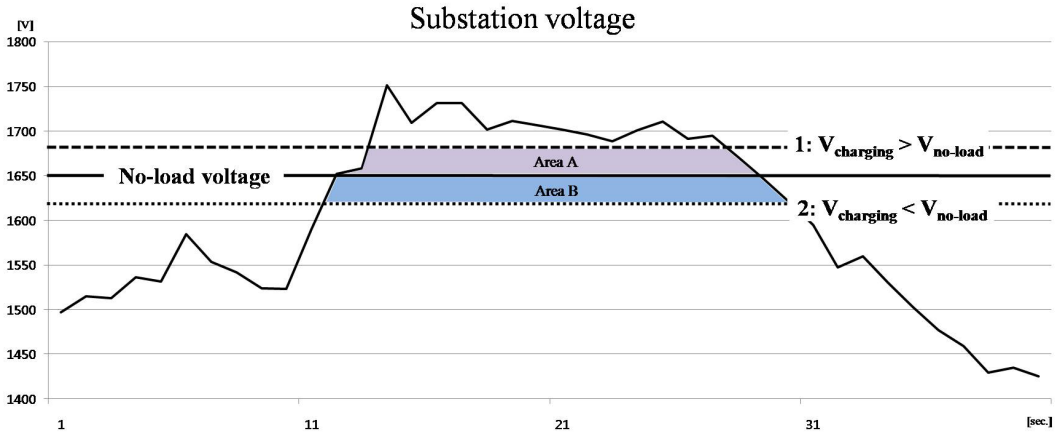

FIGURE 3. Relations between substation voltage and charging voltage

For the small load current case, when V_{sub} is slightly smaller than $V_{no-load}$, there might be unnecessary charging of the SCESs if $V_{charging}$ is set lower than $V_{no-load}$. If it is under no load condition, the SCES keep charging the power corresponding to 'Area B' in Figure 3 since V_{sub} is to be higher than $V_{charging}$. So $V_{charging}$ should be set to $V_{no-load}$ in order to store most of the regenerative power and to avoid the unnecessary charging processes.

2.2.2. *Discharging voltage determination.* Since the Korean railway system is a recurrent system, ie., the driving railway vehicles are separated by a headway time, the charged energy should be discharged within the headway to avoid energy accumulation. The total supply and energy consumption in the jth time interval can be expressed as follows:

$$P_j = \sum_i P_{ij} \tag{7}$$

$$E_j = \frac{T_{interval}}{3600} P_j \tag{8}$$

where, P_j is the power from all substation.
P_{ij} is the power from ith substation in the jth interval.
E_j is the energy from all substations in the jth time interval.
$T_{interval}$ is the time duration of each time interval.

The power balance equation in the jth time interval can be expressed as follows:

$$\sum_i P_{ij} - P_{L\_j} - P_{loss\_j} - \sum_i P_{ES\_ij} = 0 \tag{9}$$

where, P_{L_j} is the total load from all vehicles.
P_{loss_j} is the sum of the losses on the feeder and source impedance.
P_{ES_ij} is the power from the ith storage device in the jth interval.

The no-cumulative energy constraint for each SCES can be expressed as follows:

$$\sum_j \frac{1}{3600} \cdot P_{ES\_ij} = 0 \tag{10}$$

Using Equation (7) to (10), the Lagrange function on Equation (11) can be derived [16].

$$\begin{aligned} L = & \sum_j \left(\frac{T_{\text{interval}}}{3600} \cdot \left(P_j - \lambda_j \cdot \left(\sum_i P_{ij} - P_{L\_j} - P_{loss\_j} - \sum_i P_{ES\_ij} \right) \right) \right) \\ & + \sum_i \left(\lambda_{ES\_i} \cdot \sum_j \frac{1}{3600} \cdot P_{ES\_ij} \right) \end{aligned} \tag{11}$$

where, λ_{ES_i} is the Lagrange multiplier.

By solving the Lagrange function as shown in Equation (11), $V_{discharging}$ can be determined to maximize the utilization of the regenerative energy. However, in any specific railway substation, it is impossible to make a formulation of the relations between substation voltage and energy because of the diode rectifier in the substation. Since the current cannot flow into the AC power system from the DC railway system, the substation is regarded as an open circuit when the substation voltage gets higher than no-load voltage. In other words, then, substation voltage is entirely dependent upon the operation of the near substations and railway vehicles. Therefore, the gradient search iterative method had been used to find the solution as shown in Figure 4. As shown in Equation (12), the next-step $V_{discharging}$ is calculated by using values of the previous two iteration step. The iteration stops when the total amount of cumulative energy in all SCESs gets lower than

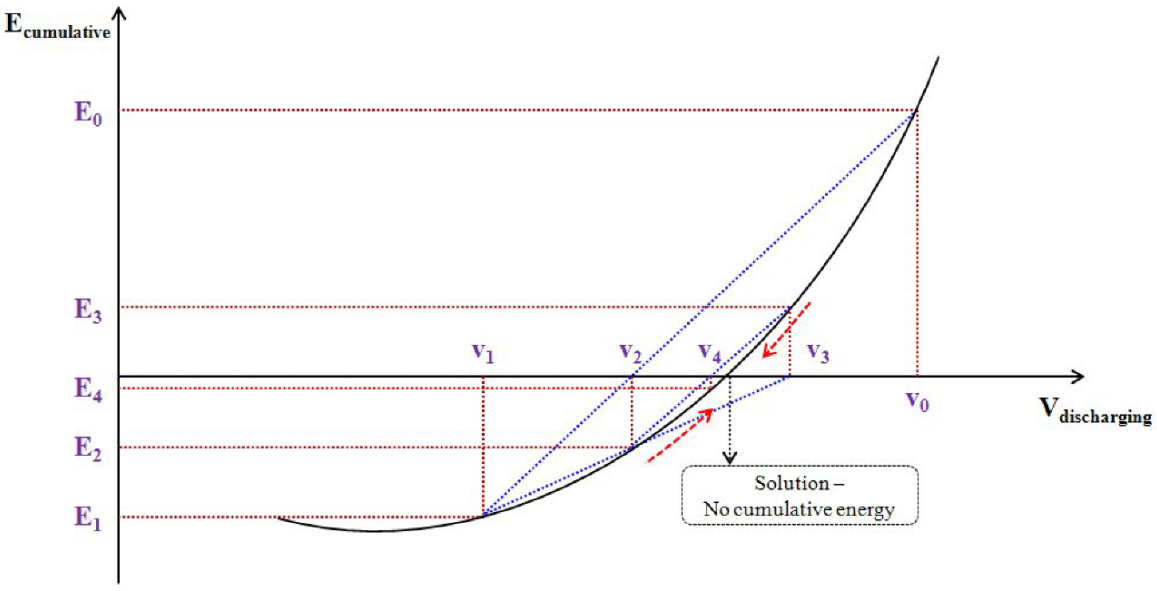

FIGURE 4. Gradient search iterative method

TABLE 1. Required data for railway powerflow analysis

Data set	Specific data	Description
Operation data	Rated voltage	
	Dwell time	Standing time in a station
	Headway	Time interval between railway vehicles
Substation data	No-load voltage	
	Source impedance	Measured impedance of substation transformer and rectifier
	Substation location	Distance of the substation from the starting point
Vehicle data	Vehicle location	Distance of the vehicle from the starting point
	Consumed power	Instantaneous power of the vehicle
Line data	Feeder impedance	Impedance per kilometer of the feeder
	Rail impedance	Impedance per kilometer of the rail

any small value as shown in Equation (13).

$$V_{i\_n+1} = V_{i\_n-1} - E_{i\_n-1} \cdot \left(\frac{V_{i\_n-1} - V_{i\_n}}{E_{i\_n-1} - E_{i\_n}} \right) \tag{12}$$

$$\sum_i |E_{i\_n}| \leq \varepsilon \tag{13}$$

2.2.3. *Flowchart of the algorithm.* In order to perform the powerflow analysis for the railway system, the algorithm needs the system operation data, the substation data, the vehicle data and the line data. The specific data and the description of each category are listed in Table 1.

Figure 5 illustrates the flowchart of the DC railway powerflow algorithm. In 'Substation & energy storage data reading', the algorithm reads the substation data set in order to find the Norton-equivalent current source parameters and to fix the substations at the specific positions. Also, efficiency and charging voltage of each SCES are read. In 'Vehicle data reading' and 'Catenary & rail data reading', the algorithm arranges the vehicles on the track using each vehicle's location information which is obtained through the train performance simulation. Based on the location information of the substations and vehicles, the algorithm performs an electric node ordering process, 'Electrical node ordering', is needed to find which two components, substation-to-vehicle or vehicle-to-vehicle, are being connected directly. Since the distance between the two components, which is being multiplied with the feeder or rail impedance per kilometer, can be converted into the impedance, the algorithm constructs the conductance matrix in 'Conductance matrix construction'.

The 'Part 1' is for the iterative solving process of powerflow. For the iterative method, it is important that an adequate initial value should be selected to reduce the calculation time. The substation and feeder voltage are designed to operate close to the rated voltage, 1,500 V. The rail voltage is designed to operate close to 0 V because the rail is connected with the ground point in the railway substation as a return path of the load current. In the iterative part, the algorithm computes the initial current vector using Equation (5) and updates the voltage vector using Equation (4). The iteration is halted when the vector distance between the pre-stepped voltage vector and the present one is smaller than any small value, ε.

$$G_{swapped} \cdot \begin{bmatrix} I_{sub1} + I_{ES1} \\ V_{sub2} \\ V_{feeder} \\ V_{rail} \end{bmatrix} = \begin{bmatrix} V_{sub1} \\ I_{sub2} + I_{ES2} \\ -I_{veh} \\ I_{veh} \end{bmatrix} \tag{14}$$

The energy storage analysis part of the flowchart in 'Part 2' in Figure 5 has the same calculation sequence with the 'Part 1'. However, since the variables which are to be derived should be swapped, the Equation (4) is changed as shown in Equation (14) with the assumption that the first railway substation needs the energy storage operation. Through the iteration for the modified equation, the storage current and feeder voltage of each railway substation can be calculated.

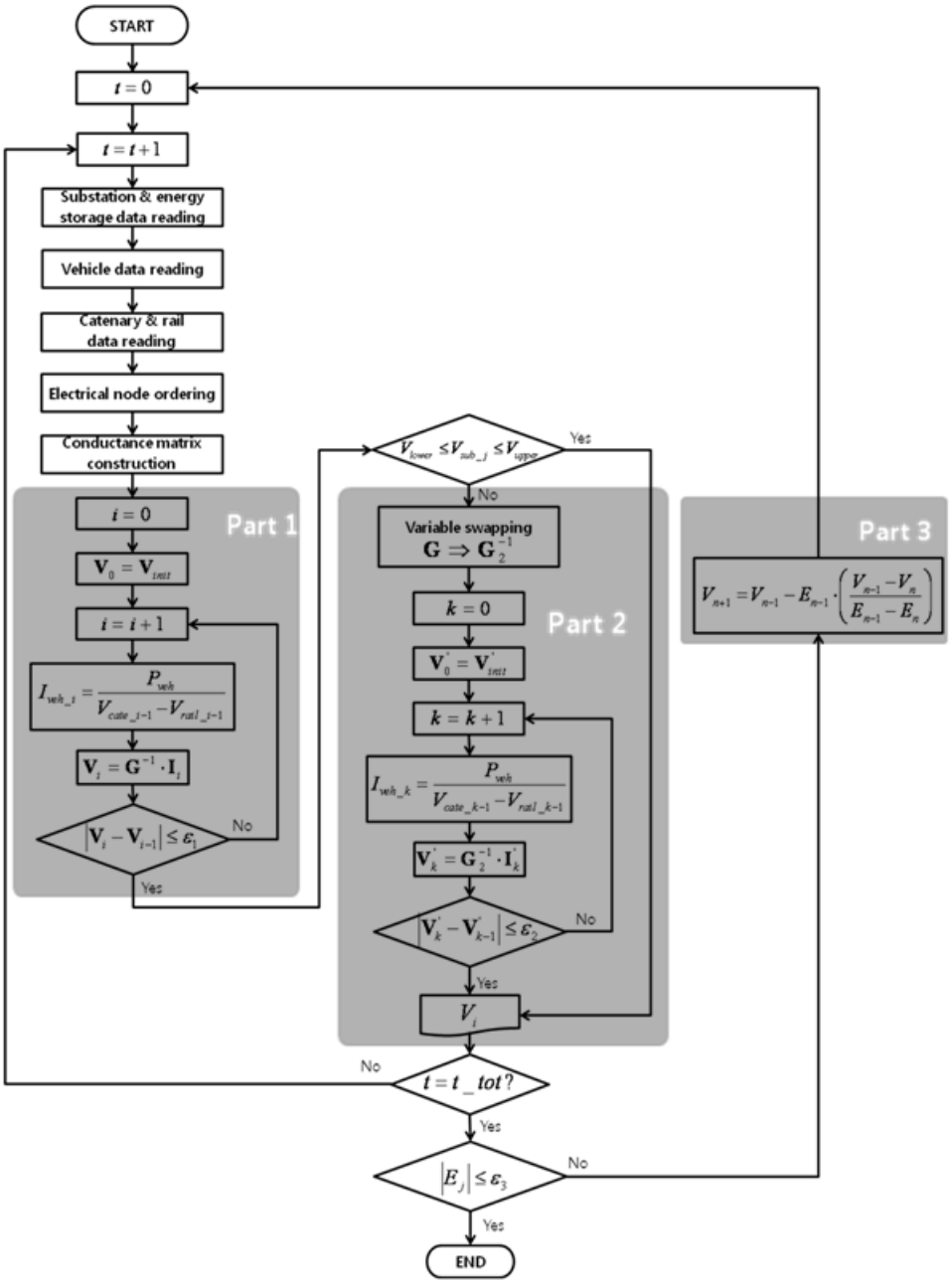

FIGURE 5. Flowchart of the powerflow algorithm with storage optimization algorithm

TABLE 2. Stations and substations location data on the Seoul Metro Line 7

Station name	Location (m)	Sub. No.	Station name	Location (m)	Sub. No.
Jangam	0		Gangnam-gu Office	21,565	
Dobongsan	1,056		Hak-dong	23,478	
Suraksan	2,315	Sub 1	Nonhyeon	24,818	Sub 8
Madeul	3,894		Banpo	25,418	
Nowon	5,315		Express Bus Terminal	26,534	
Junggye	6,155	Sub 2	Naebang	28,758	Sub 9
Hagye	7,140		Isu	29,838	
Gongneung	8,470		Namseong	30,592	Sub 10
Taerueng	9,320	Sub 3	Soongsil	32,783	
Meokgol	9,720		Sangdo	33,675	Sub 11
Junghwa	11,120		Jangseungbaegi	34,696	
Sangbong	12,090	Sub 4	Sindaebangsamgeri	35,767	
Myeonmok	12,950		Boramae	36,791	Sub 12
Sagajeong	14,071		Sinpung	37,401	
Yongmasan	14,951		Daerim	38,858	
Junggok	15,792	Sub 5	Namguro	40,035	Sub 13
Gunja	16,752		Gasan Digital Complex	40,575	
Childrel's Grand Park	17,633		Cheolsan	42,195	Sub 14
Konkuk Univ.	18,422	Sub 6	Gwang-myeongsageori	43,655	
Ttukseon Resort	19,608		Cheonwang	45,115	Sub 15
Cheongdam	21,115	Sub 7	Onsu	47,095	Sub 16

To find the solution without the voltage-energy formulation, the gradient search iterative method has been used as shown in 'Part 3' in Figure 5 to find the optimized discharging voltage of each SCES. It selects any two initial points and calculates the next point using the gradient between the two initial points based on the Equation (12). The iteration stops when the cumulative energy gets lower than any small value, ε, as shown in Equation (13).

3. **Test System.** Amongst the 13 Korean suburban railway lines, the SCES-considered powerflow analysis has been performed for the Seoul Metro Line 7 since it is the largest system in Korean suburban railway systems. The Seoul Metro Line 7 is composed of 42 stations and 16 substations. The name and the distance information for each station are listed in Table 2. The first station, *Jangam*, is set to the starting point, 0 [m]. Also, the location and distance from the *Jangam* station of the railway substations in Line 7 are listed in Table 2. The substations had been installed for every 2-4 km with considering voltage drop. From the location of *Onsu* station, the total track length is 47.095 km.

Seoul Metro Line 7 is designed to operate with the 1500 V rated voltage considering the voltage drop across the source impedance, 0.02956 Ohm. Resistance values per unit length, 1 km, of the equivalent conductors for the feeder and rail are 0.0203 and 0.000464 Ohm/km, respectively. Since the case studies assume rushhour, the headway time is 180 seconds. Considering headway and the total operation time, the maximum number of railway vehicles is to be 24 on each direction. Since the powerflow algorithm considers 16 substations and 48 vehicles, the dimension of system conductance matrix is to be 112 by 112. Based on the system and operating conditions, the powerflow input data are listed in Table 3.

TABLE 3. Powerflow input data of Seoul Metro Line 7

Specific data	Seoul Metro Line 7
Rated voltage	1,500 [V]
Dwell time	30 [sec]
Total operation time	4,161 [sec]
Total track length	47,095 [m]
Headway	180 [sec]
Max. # of vehicles	24
No-load voltage	1,650 [V]
Source impedance	0.02956 [Ω]
Feeder impedance per km	0.0203 [Ω/km]
Rail impedance per km	0.000464 [Ω/km]

TABLE 4. Simulation condition for case studies

	No SCES	SCESs			
Cases	Case 1	Case 2	Case 3	Case 4	Case 5
$V_{charging}$ (V)	–	1637.5	1650.0	1662.5	1675.0

4. **Case Studies.** Case studies had been performed for various simulation conditions as shown in Table 4. Case 1 is for the case which does not consider SCESs and Case 2 to 5 consider SCESs with 4 kinds of operation strategies. These four cases are to verify whether the SCESs improve energy efficiency of the railway system by comparing with Case 1. The charging voltage in Case 4 or 5 is set to higher than no load voltage. Comparing with Case 3, this condition is to verify whether the regenerative energy is utilized completely or not. Case 2 is to compare energy capacity of SCESs with Case 3 of which charging voltage is set to no load voltage under the condition of full utilization of regenerative energy.

Through the SCES capacity optimization powerflow algorithm which is shown in Figure 5, simulation has been performed for 5 cases shown in Table 4. This algorithm calculates the discharging voltage, instantaneous power, and needed energy capacity of each SCES. In the aspect of the system, the total energy supply, consumption and energy efficiency are also calculated.

For the 4 cases considering SCESs, the discharging voltage of each SCES is listed in Table 5. This shows that the higher charging voltage makes the discharging voltage lower. Since the regenerative cannot be charged with high charging voltage condition, it is obvious that the voltage to discharge the total charged energy in an SCES is calculated lower value.

Based on the discharging voltage of each SCES in Table 5, the energy capacity of each SCES had been calculated as shown in Table 6. The energy capacity is estimated from the difference between maximum and minimum values of cumulative energy. Table 6 shows that the higher charging voltage makes the needed energy capacity lower. Since the high charging voltage means small regenerative energy charging, it is obvious that the energy capacity of each SCES is calculated smaller value.

System energy efficiency analysis for the 5 cases is listed in Table 7. Through an analysis for the Table 7, three kinds of discussions had been derived as below:

1. How the SCESs effect on the energy efficiency of the electric railway system.

TABLE 5. Calculated discharging voltage of each SCES

Substation name	Calculated $V_{discharging}$ [V]			
	Case 2 (1637.5)	Case 3 (1650.0)	Case 4 (1662.5)	Case 5 (1675.0)
Suraksan	1601.81	1582.24	1563.98	1541.58
Junggye	1616.99	1610.42	1602.06	1588.76
Taerueng	1616.14	1601.58	1588.76	1570.96
Sangbong	1615.94	1600.89	1586.21	1569.51
Junggok	1620.61	1608.73	1596.78	1588.78
Konkuk Univ.	1622.92	1610.95	1596.49	1584.09
Cheongdam	1622.24	1612.65	1596.11	1587.71
Nonhyeon	1614.63	1602.79	1591.40	1579.40
Naebang	1620.72	1609.33	1597.49	1589.19
Namseong	1624.03	1614.36	1604.31	1597.41
Sangdo	1618.66	1595.05	1576.73	1566.43
Boramae	1623.70	1611.24	1596.22	1589.40
Namguro	1623.69	1612.22	1600.56	1589.46
Cheolsan	1629.42	1600.53	1567.37	1570.90
Cheonwang	1633.72	1620.32	1608.74	1593.74
Onsu	1637.50	1630.46	1617.06	1599.04

TABLE 6. Energy capacity of each SCES

Substation name	Energy capacity of each SCES [kWh]			
	Case 2	Case 3	Case 4	Case 5
Suraksan	29.84	21.10	13.28	7.04
Junggye	20.37	16.87	14.32	7.01
Taerueng	49.47	36.83	31.33	21.65
Sangbong	91.37	71.59	56.78	41.30
Junggok	52.16	45.01	41.18	33.51
Konkuk Univ.	25.68	16.96	9.85	7.01
Cheongdam	62.50	34.36	11.06	7.31
Nonhyeon	61.39	49.14	39.60	30.21
Naebang	59.22	42.57	26.18	13.58
Namseong	33.72	18.70	12.21	6.93
Sangdo	63.00	31.86	15.46	5.99
Boramae	28.43	14.10	6.96	4.83
Namguro	62.02	42.18	25.82	15.99
Cheolsan	45.05	14.21	2.19	0.48
Cheonwang	46.10	11.33	3.54	0.85
Onsu	27.26	13.48	5.52	1.41
Total capacity	**757.58**	**478.29**	**315.28**	**205.09**

2. Why the $V_{charging}$ should not be set higher than $V_{no-load}$, that is, what the problem is with the $V_{charging}$ which is higher than $V_{no-load}$.
3. Why the $V_{charging}$ should not be set lower than $V_{no-load}$, that is, what the problem is with the $V_{charging}$ which is lower than $V_{no-load}$.

4.1. **Analysis for simulation results.** As shown in Table 7, it can be found that the SCESs are good at saving energy. Before SCESs consideration, the system efficiency is

TABLE 7. Simulation results for the 5 cases (1 hour)

Cases	No SCES	SCESs			
	Case 1	Case 2	Case 3	Case 4	Case 5
$V_{charging}$ [V]	–	1637.5	1650.0	1662.5	1675.0
Total supply [MWh]	25.471	18.443	18.397	21.074	22.590
Total load [MWh]	16.706	16.706	16.706	16.706	16.706
Energy efficiency [%]	**65.588**	**90.582**	**90.808**	**79.273**	**73.953**
Energy saving [MWh]	–	7.028	7.074	4.397	2.881
Energy saving rate [%]	–	27.593	27.773	17.263	11.311
Total SCES capacity [kWh]	–	**757.58**	**478.29**	315.28	205.09

– Energy efficiency = (Total load) / (Total supply) $*$ 100 (%)
– Saving rate = (Energy saving) / (Total supply without SCESs) $*$ 100 (%)

65.588%. However, installation of SCESs improves the efficiency to 90.808% maximum by storing the regenerative energy and releasing it when the system needs. According to the operation boundary of SCESs, since the utilization rate of regenerative energy of each case is different, it is noticed that the energy saving and saving rate are indicated differently. In Table 7, the energy efficiency is calculated from the total supply and total load. As mentioned before, since the railway loads are constant power loads, same amount of total load, 16.706 MWh, are applied to all cases.

4.1.1. $V_{charging} > V_{no-load}$. Compared with Cases 4 and 5, Cases 2 and 3 indicate high improvement in energy saving and efficiency. Since the SCESs in Cases 4 and 5 are not set to charge between the $V_{no-load}$ and $V_{charging}$, the regenerative energy cannot being utilized completely. The still unutilized regenerative energy is dissipated as thermal losses.

4.1.2. $V_{charging} < V_{no-load}$. Compared with Case 2, it is found that the almost same amount of energy saving is being achieved. However, since there are unnecessary charging operations between $V_{no-load}$ and $V_{charging}$ in Case 2, it is noticeable that the bigger capacity of SCESs is being needed. Also, the system loss is being increased because of the loss on the equivalent impedance of the source and SCESs during unnecessary charging operations.

4.2. **Optimal case: Case 3.** Case 3 indicates the optimal performance to improve the energy efficiency of the electric railway system and has the minimized storage capacity of SCESs. It performs the full-utilization of the regenerative energy and no-unnecessary charging operations. Table 8 illustrates the results of the maximum current and the instantaneous power of each SCES in Case 3. These values can be applied to determine the power capacity of switching devices, DC-to-DC converter.

Among the 16 SCESs in each railway substation, since the SCES in *Sangbong* substation indicates the largest capacity, more detailed analysis for it has been performed below. As shown in Table 5, the discharging voltage of *Sangbong* SCES is 1600.89 V. Therefore, as shown in Figure 6, the feeder voltage is limited within 1600.89 V and 1650.0 V by the charging and discharging operation. When the feeder voltage goes over 1650.0 V, that is, the regenerative energy is concentrated to *Sangbong* substation, SCES drives charging circuit to absorb the current surplus, and vice versa. Although the feeder voltage is between voltage limits, two voltage plots are not exactly same. This is due to the operation of nearby SCESs. Since the Korean DC electric railway employs the parallel dispatch, the performance of substation or SCES affects the voltage or power of nearby substation voltage.

TABLE 8. Power capacity and maximum current of SCESs in Case 3

Substation name	Each SCES of the Case 3	
	Maximum current [A]	Power capacity [kW]
Suraksan	4602.21	2022.72
Junggye	3005.45	1377.50
Taerueng	6356.97	2828.11
Sangbong	7591.43	3375.85
Junggok	5387.93	1469.47
Konkuk Univ.	3524.56	1615.42
Cheongdam	3759.61	1723.15
Nonhyeon	6846.44	3052.84
Naebang	3710.72	1700.75
Namseong	3267.59	1465.30
Sangdo	4926.81	2258.12
Boramae	5332.50	2386.65
Namguro	5609.35	2570.95
Cheolsan	3169.40	1409.09
Cheonwang	3189.61	1435.61
Onsu	3610.34	1635.14

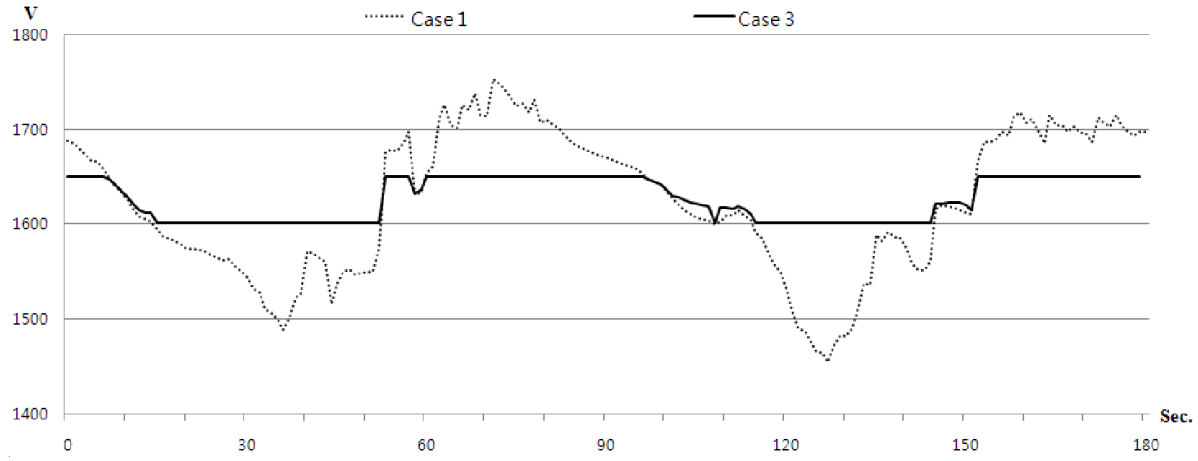

FIGURE 6. Feeder voltage of *Sangbong* substation in Case 1 and 3

Figures 7 and 8 illustrate the instantaneous power and cumulative energy of *Sangbong* SCES. In Figure 7, the positive power indicates the energy charging, and vice versa. As shown in Table 8, the power capacity of converter for *Sangbong* SCES should be 3.376MW as least. This power capacity of DC-to-DC converter is a primary factor as important as the energy capacity to determine the cost. In Figure 8, the maximum and minimum cumulative energy are 13.16 and –40.54kWh, respectively. In other words, it should have 53.70kWh at least as usable energy capacity. In the case of SCES, since it can use 75% energy capacity of its total storage capacity, its actual capacity should be 71.59kWh as shown in Table 8. The *Sangbong* SCES has two charging-discharging cycles in headway. That is, it experiences 40 cycles in an hour. This implies that the SCES is good to be applied on the electric railway system since it has long lifecycle.

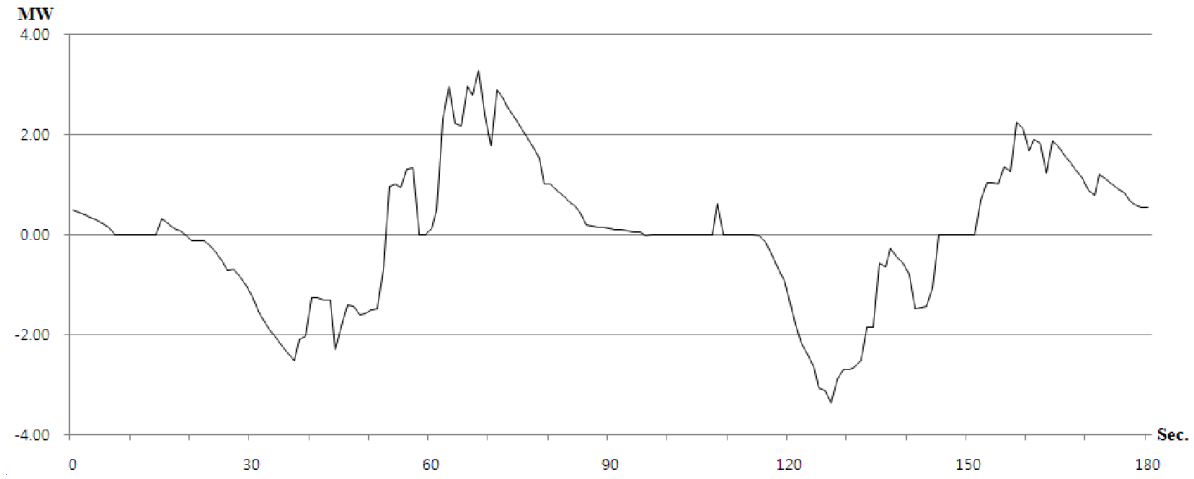

FIGURE 7. Instantaneous power of SCES in *Sangbong* substation for Case 3

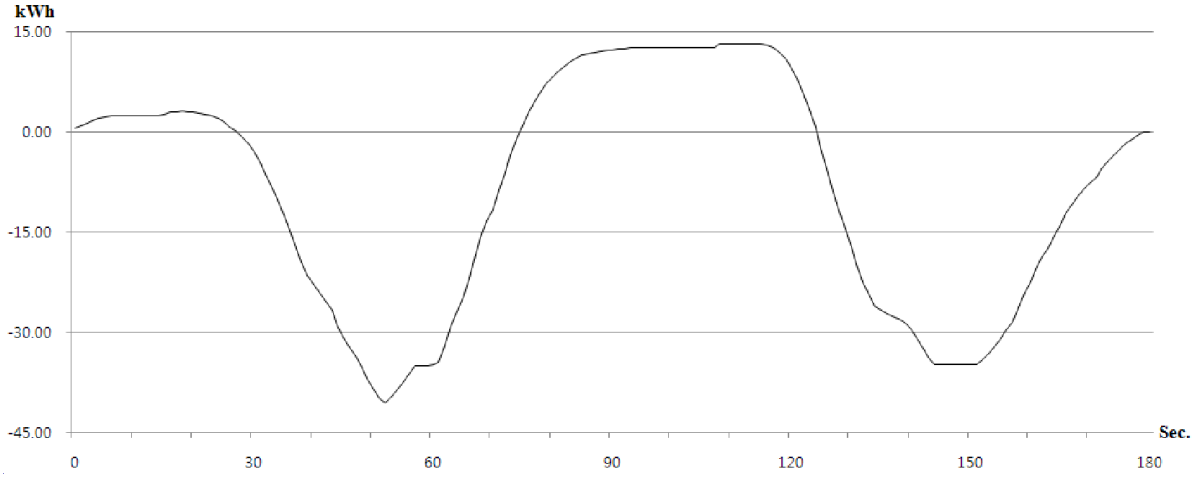

FIGURE 8. Cumulative energy of SCES in *Sangbong* substation for Case 3

5. **Conclusions.** In this paper, a DC railway powerflow algorithm which can derive not only the substation voltage and system powerflow but also the optimal power and storage capacity of SCESs have been developed. The optimal power and storage capacity of SCESs can be found by using Lagrange optimization and gradient search iterative method. This optimization algorithm can determine the optimal charging and discharging operation boundary for each SEES with the no-cumulative energy constraints and calculate the capacity with those operation boundaries.

To verify the algorithm, the case studies have been performed through the whole part of Section 5. For the several charging voltage conditions, the discharging voltage on each SCES is determined and the effect of energy efficiency improvement of SCESs has been analyzed. A summary of case studies is as follows:

- SCESs can improve the energy efficiency of the DC railway system significantly.
- The regenerative energy cannot be utilized completely with the charging voltage which is higher than no load voltage.
- The overabundance of SCES storage capacity might be induced without efficiency improvement anymore when the charging voltage is lower than no load voltage.

A quantitative analysis for the optimal case, Case 3, has been performed. The SCESs can improve the efficiency to over 90% and save 7.074 MWh for 1 hour. The total amount

of energy saving means a reduction in the operation cost of 27.77%. Then, the amount of total required ESS capacity is 478.29 kWh. Additionally, the SCESs can stabilize the feeder voltage within the voltage limits, charging and discharging voltage, thus avoiding transient overvoltage or undervoltage. Based on this algorithm in this paper, it is expected that enhanced algorithm which can maximize 'return of investment (ROI)' and suggest optimal investment strategy with limited budget can be developed.

Acknowledgment. This work was supported by National Research Foundation of Korea Grant funded by the Korean Government (20100018462).

REFERENCES

[1] J. Skea, D. Anderson, T. Green, R. Gross, P. Heptonstall and M. Leach, Intermittent renewable generation and maintaining power system reliability, *IET Gener. Transm. Distrib.*, vol.2, no.1, pp.82-89, 2008.

[2] B. Bletterie and H. Brunner, Solar shadows, *Power Engineer*, vol.20, no.1, pp.27-29, 2006.

[3] G. P. Harrison and A. R. Wallace, Optimal power flow evaluation of distribution network capacity for the connection of distributed generation, *IET Gener. Transm. Distrib.*, vol.152, no.1, pp.115-122, 2005.

[4] J. S. Bak, H. L. Yang, Y. K. Oh, Y. M. Park, K. R. Park, C. H. Choi, W. C. Kim, J. W. Sa, H. K. Kim and G. S. Lee, Current status of the KSTAR construction, *Cryogenics*, vol.47, no.7-8, pp.356-363, 2007.

[5] T. M. Weis and A. Ilinca, The utility of energy storage to improve the economics of wind-diesel power plants in Canada, *Renew. Energy*, vol.33, no.7, pp.1544-1557, 2008.

[6] F. Barbir, T. Molter and L. Dalton, Regenerative fuel cells for energy storage: Efficiency and weight trade-offs, *IEEE Aerosp. Electron. Syst. Mag.*, vol.20, no.5, pp.35-40, 2005.

[7] R. J. Hill, Y. Cai, S. H. Case and M. R. Irving, Iterative techniques for the solution of complex DC-rail-traction systems including regenerative braking, *IET Gener. Transm. Distrib.*, vol.143, no.6, pp.613-615, 1996.

[8] A. Adinolfi, R. Lamedica, C. Modesto, A. Prudenzi and S. Vimercati, Experimental assessment of energy saving due to trains regenerative braking in an electrified subway line, *IEEE Trans. on Power Deliv.*, vol.13, no.4, pp.1536-1542, 1998.

[9] L. Battistelli, F. Ciccarelli, D. Lauria and D. Proto, Optimal design of DC electrified railway stationary storage system, *International Conference on Clean Electrical Power*, pp.739-745, 2009.

[10] M. Steiner and J. Scholten, Energy storage on board of DC fed railway vehicles, *IEEE the 35th Annual Power Electronics Specialists Conference*, vol.1, pp.666-671, 2004.

[11] M. Yano, M. Kurihara and S. Kuramochi, A new on-board energy storage system for the railway rolling stock utilizing the overvoltage durability of traction motors, *The 13th European Conference on Power Electronics and Applications*, 2009.

[12] B. Y. Ku and J. S. Liu, Solution of DC power flow for non-grounded traction systems using chain-rule reduction of ladder circuit Jacobian matrices, *ASME/IEEE Joint Railroad Conference*, pp.123-130, 2002.

[13] H. Lee, *A Study on Modeling for 1500V DC Power-Supplying Railroad System Using EMTDC*, Master Thesis, Korea University, 2005.

[14] H. Lee, J. Song, C. Lee, H. Lee, G. Jang and G. Kim, DC Loadflow method considering movement of electric vehicles, *The 6th International Symposium on Management Engineering*, 2009.

[15] H. Lee, H. Lee, C. Lee, G. Jang and G. Kim, Energy storage application strategy on DC electric railroad system using a novel railroad analysis algorithm, *J. Elec. Eng. & Tech.*, vol.5, no.2, pp.228-238, 2010.

[16] A. J. Wood and B. F. Wollenberg, *Power Generation, Operation, and Control*, 2nd Edition, Wiley, 1996.